POLITECNICO DI TORINO
Repository ISTITUZIONALE

Reflectance-based low-cost disposable optical fiber surface plasmon resonance probe with enhanced biochemical sensitivity

Terms of use:

Publisher copyright

(Article begins on next page)

01 September 2025

Reflectance-based low-cost disposable optical fiber surface plasmon resonance probe with enhanced biochemical sensitivity

Papiya Dhara
Vinod Kumar Singh
Massimo Olivero
Guido Perrone

Reflectance-based low-cost disposable optical fiber surface plasmon resonance probe with enhanced biochemical sensitivity

Papiya Dhara,[a,b,*] **Vinod Kumar Singh,**[a] **Massimo Olivero,**[b] **and Guido Perrone**[b]
[a]Indian School of Mines, Department of Applied Physics, Dhanbad 826004, India
[b]Politecnico di Torino, Department of Electronics and Telecommunications, 24 Corso Duca degli, Abruzzi, Torino 10129, Italy

Abstract. A reflectance-based surface plasmon resonance (SPR) fiber sensor with enhanced sensitivity for biochemical sensing is reported after comparing its result with the transmittance-based SPR optical fiber sensors. The fabricated SPR sensor contains a gold-coated multimode fiber with the implementation of a standard source-sensor-spectrometer interrogation system. As the refractive index of the liquid under test is increased, a redshift of the SPR is observed. The coupling of the source to the fiber sensor is optimized by investigating the effect of an intentional misalignment in transmission-based setup. When a fiber tip coated with the silver mirror and the bifurcated fiber bundle is used, an alignment-free disposable sensor probe is achieved. A comprehensive characterization of the proposed reflectance-based SPR probe is discussed. The maximum sensitivity of 3212.19 nm/refractive indexunit (RIU) is obtained. © *2016 Society of Photo-Optical Instrumentation Engineers (SPIE)* [DOI: 10.1117/1.OE.55.4.046114]

Keywords: sensors; surface plasmon resonance; fiber optic sensors; biochemical sensors; reflectance-based fiber sensor; bifurcated fiber bundle.

Paper 160221 received Feb. 16, 2016; accepted for publication Apr. 5, 2016; published online Apr. 26, 2016.

1 Introduction

In the field of optoelectronics, optical fibers have been used in various sensor fields as it has some unique advantages over other optoelectronic sensors, such as low fabrication cost, small, robust, high accuracy, multiplexing, remote sensing, high flexibility, low propagation loss, high sensitivity, and immunity to electromagnetic interference. In recent times, fiber is utilized as temperature, strain, pressure, rotation, displacement, refractive index (RI), polarization, ultrasound, vibration, viscosity, turbidity, humidity, water level, and so on, parameter sensors.[1–5] The spectroscopic absorption sensing platform has been proposed to combine the photonic crystal fiber (PCF) and long-period grating (LPG) as a gas sensor.[6] A PCF–LPG humidity sensor has been designed with high sensitivity and selectivity for detection of moisture ingression into structures. Two types of nanofilms have been coated on the surface of air channels in the grating region by electrostatic self-assembly deposition method to enhance sensitivity.[7] The LPGs have been incorporated in PCF to investigate sensitivity to the external conditions, such as temperature, strain, RI of the surroundings, curvature, and torsion.[8] It has been revealed by experiment that the nanofilm-coated LPGs are more sensitive to moisture in terms of both wavelength shift and resonance intensity change.[9] Optical sensor based on nonlinear effect has introduced stimulated Brillouin scattering into the instantaneous microwave frequency measurement system.[10,11]

Surface plasmon resonance (SPR)-based fiber optic sensor is one of the promising sensing techniques for real-time detection and monitoring of chemical properties of material. In the search of more convenient and cost-effective SPR sensors, the traditional prism-based systems have been replaced by a fiber optic design.[12] Gold is the traditional material used to produce the thin film for SPR as it has high chemical resistance. During the past two decades, SPR-based sensors have been employed for label-free, real-time analysis of different biological concentrations, such as antibody, antigen, and so on, and chemical concentrations.[13,14] Two convenient ways have been proposed to detect the SPR signal. In the first type, the light from a broadband source is launched into the fiber through one of the ends and the SPR spectrum of the transmitted light is recorded at the other end, which is the so-called transmission-based setup.[15–17] In the transmission-based setup, the authors have proposed a preliminary version of a differential SPR-based sensor specifically designed for permanent monitoring, mainly in the areas of environment and safety.[18,19] The unwanted impacts in long-term monitoring are perturbations from the mechanical setup or drifts in the electronic circuits or misalignment between source/detector and coated optical fiber. So, it is of utmost importance that we should fabricate a thin-film-coated biosensor, which can be used easily for real-time stable measurement without any restrictions and hence could be used in a beneficial and user-friendly way in our daily life. The other mechanism to detect SPR signal is done by launching the light from a broadband source into the sensing fiber through one of its ends and the SPR spectrum of the transmitted light is recorded after reflection through the other end of the receiving fiber, which is called reflection-based setup. The real-time label-free immunoassay by gold nanoparticles coated optical fiber having fast detection time, high resolution, and sensitivity have been established by the reflection-based setup.[20,21] To achieve reflection-based sensing probe, silver mirror is

coated at the distal end of the fiber, which enhances performance for RI measurement.[22] Researchers generally use a coupler to launch and detect the light path, which could introduce interference in transmission spectra.[2,23] Fiber bundle has been used to collect the reflected and scattered light to sense turbidity of the liquid.[24] Bifurcated fiber bundle has been investigated as an optical displacement sensor from a theoretical perspective.[25] The light has been guided through the bifurcated optical fiber to a flow-through cell and luminescence has been collected to the photometer through the output bundle to sense biochemicals.[26] The optical properties of human whole blood and blood plasma have been characterized in the near-infrared region using a double integrating sphere technique. This range of wavelength, which is called a tissue window, is important as it allows for deeper penetration in applications, such as photoacoustics, photodynamic therapies, and optical imaging.[27,28] Zhernovaya et al.[29] have proposed the direct RI measurement of human deoxygenated and oxygenated hemoglobin in the visible range due to its importance for medical diagnostics and treatment.

In this study, gold-coated multimode fiber (MMF) has been used in transmission and reflection-based setup for detection of different RIs of liquid from 1.33 to 1.35. In order to reduce the inconvenience of disposable use of the transmission setup, the sensing probe has been fabricated by a suitable fiber component for reflection-based setup, which is alignment-free. The sensor probe has been coated with silver mirror at the distal end of the fiber tip to increase reflectivity as well as sensitivity within the range of 1.33 to 1.37 of RI. To get an accurate evaluation of the SPR wavelength, output curves have been fitted using a Lorentzian function. The replacement of transmittance-based sensor with reflectance-based SPR fiber sensors has been established by using bifurcated fiber bundle to detect biochemicals. Recently, Qazwinia et al.[30] have proposed the sensitivity of the gold-coated tapered fiber SPR probe in the range of 1600 to 2000 nm/refractive index unit (RIU). In this work, the sensitivity has been ∼3212.19 nm/RIU for biochemical detection.

2 Theoretical Background

SPR is a resonance due to the collective oscillation of the electrons at the metal-dielectric (or analyte) interface stimulated by incident p-polarized light. This kind of electron density oscillation is also known as surface plasmon wave (SPW). When the p-polarized light is incident in a such way that the propagation constant (and energy) of resultant evanescent wave is equal to that of the SPW, there will be an absorption of energy and a sharp dip will be visible at a particular wavelength of output signal, which is called resonance wavelength. The so-called resonance condition is[19]

$$kn_c \sin \theta = k\sqrt{\frac{\varepsilon_{mr}n_s^2}{\varepsilon_{mr} + n_s^2}}; \qquad k = \frac{2\pi}{\lambda}. \qquad (1)$$

The left-hand side term is the propagation constant of the evanescent wave produced as a result of attenuated total reflection of the light incident at an angle θ through an optical fiber of core RI n_c. The right-hand term is the SPW propagation constant, with ε_{mr} as the real part of the metal–dielectric constant (ε_m) and n_s as the RI of the sensing (or dielectric) layer. This condition is very sensitive to

minimum change in the surrounding. The performance of SPR sensors is determined by three parameters: sensitivity, signal-to-noise ratio (SNR), and resolution.[31]

Sensitivity of an SPR sensor is defined as how much the resonance wavelength shifts ($\delta\lambda_{res}$) with a change in RI (δn_s) of the sensing layer. So, the sensitivity (S_n) of the sensor with spectral interrogation is expressed as

$$s_n = \frac{\delta\lambda_{res}}{\delta n_s} \ (nm/RIU). \qquad (2)$$

The SNR (N) precisely determines the accuracy of the sensor. The narrower the spectral bandwidth, the higher will be the detection accuracy. Then, the SNR can be presented as

$$SNR(N) = \left[\frac{\delta\lambda_{res}}{\delta\lambda_{sw}}\right]_n, \qquad (3)$$

where $\delta\lambda_{SW}$ is the full width at half maximum (FWHM) of SPR curve.

The resolution (ΔN) of the SPR-based optical sensor is the minimum amount of change in RI detectable by the sensor. The resolution can be expressed as

$$\Delta N = \frac{\delta n_s}{\delta\lambda_{res}} \delta\lambda_{DR}, \qquad (4)$$

where $\delta\lambda_{DR}$ is the spectral resolution of the spectrometer, which is used to measure the resonance wavelength.

The working principle of the bifurcated fiber bundle is based on the following assumptions:

- The bifurcated fiber bundle in front of the mirror is situated as a set of two independent parallel equal fibers contacting each other with no space left between them. Both the transmitting and receiving fibers have perfectly circular cross-sections with area S_a and radius W_a.
- The light leaving the transmitting fiber is represented by a perfectly symmetrical cone with angle of divergence θ.

By Gaussian beam approach, normalized power collected by the receiving fiber is

$$P_N = \frac{P}{P_{max}} = \frac{8}{\tau^2} \ \exp\left(1 - \frac{8}{\tau^2}\right), \qquad (5)$$

where τ is the dimensionless parameter related to radius W_a.

$$\tau = 1 + 2h_N, \qquad (6)$$

where h_N is the normalized distance between mirror surface being monitored and end fiber. If $h_N \rightarrow 0$, the value of collected power will increase.
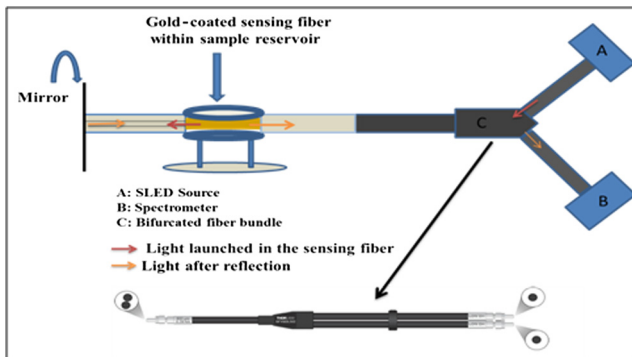
3 Experimental Section

3.1 Fabrication of Gold-Coated Surface Plasmon Resonance Sensor and Experimental Setup

The fiber chosen for validation experiments is $400 \pm 8 \ \mu m$ silica core diameter MMF with tetraethyl orthosilicate polymer cladding, 0.39 NA fiber (Thorlabs, FT400EMT), for the
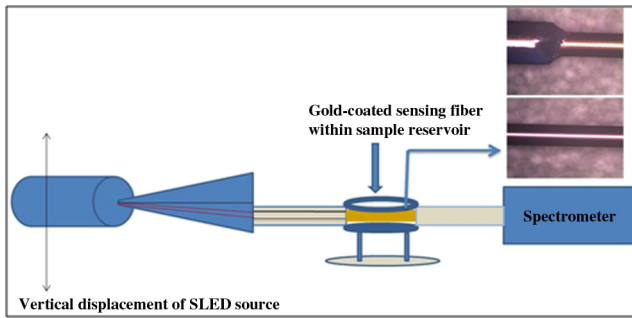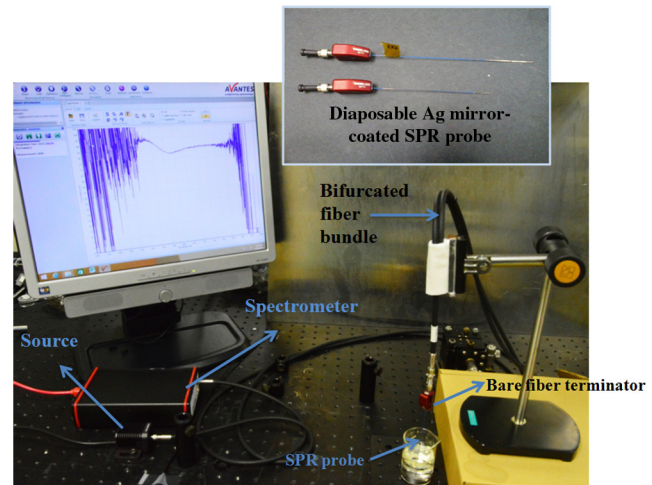
Fig. 1 Transmission-based optical fiber SPR sensor setup with intentional vertical misalignment, microscopic image of gold-coated MMF (inset), SLED = super luminescent emitting diode.

**Fig. 2** Reflection-based optical fiber SPR sensor setup.

Fig. 4 The reflectance-based Ag mirror coated SPR probe setup; inset shows disposable Ag mirror coated SPR probe connected with bare fiber terminator.

simplicity in handling and coupling. The gold layer of (50 ± 4) nm thickness has been deposited on the exposed core for a length of 2 cm using an radio frequency assisted plasma sputtering machine. The transmission-based setup is shown as a schematic diagram in Fig. 1, where the source of SPR generation is the broadband light-emitting diode (LED) source (470 to 850 nm) with constant current supply ≈ 200 mA, attached with a spectrometer of resolution 0.3 nm as detector. The microscopic images of the gold-coated fiber are shown in the inset of Fig. 1. As shown in Fig. 2, the bifurcated fiber bundle (BFY200LS02, Thorlabs) has been used to launch the

light through coated fiber and receive the SPR spectrum of the transmitted light after reflection by the bulk mirror in the reflection-based setup. The bifurcated fiber bundle has been used instead of optical fiber coupler to decrease coupling loss of light. A plane mirror has been installed at the distal end of the fiber for reflection of the SPR spectrum of the transmitted light. The probe has been fabricated by connecting the gold-coated fiber with a bare fiber terminator (BFT1, Thorlabs). The fiber terminator makes the probe disposable, which is very essential for biomedical applications. To make the SPR probes more sensitive, the tip of the gold-coated fibers has been coated subsequently with a thin silver mirror. The silver mirror coating has been realized by using a chemical technique with Tollen's reagent.[32] After silver coating, the reflectance of the SPR probe has been increased by 90% in comparison with using bulk mirror as shown in Fig. 3. It is also predictable by the microscopic images of the fiber tip that the light reflected from the Ag mirror coated fiber tip has high reflectance than uncoated fiber.

The reflection-based setup with Ag mirror coated SPR probe has been shown in Fig. 4, where the same source
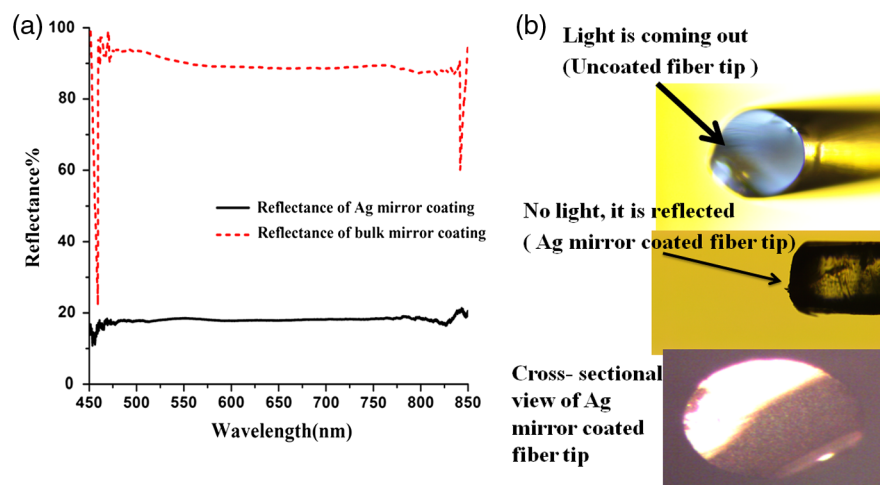
Fig. 3 Reflectance of SPR probe in comparison with bulk mirror. (a) The reflectance variation of Ag mirror coated SPR probe and bulk mirror SPR probe and (b) the microscopic images of Ag mirror coated fiber tip with cross-sectional view.

and detector have been used as the above setup. The Ag mirror coated SPR probes have been connected with bare fiber terminator, which transforms it into disposable as shown in the inset image of Fig. 4.

3.2 Experimental Procedure

The solutions prepared with proper mixing of glycerol–water and pure water have been utilized as different RIs sample as presented in Table 1, and these sets of solution have been used in the transmission-based setup and reflection-based setup with bulk mirror experiment to compare their sensitivity.

Another set of solutions has been prepared with proper mixing of sugar–water in weight/volume% concentration and pure water to use it as the different RIs sample in reflection-based Ag mirror coated SPR probe experiment as presented in Table 2. During a sensing experiment in transmission- and reflection-based setup with bulk mirror, the analytic solution has been injected into the chamber and 100 measurements have been acquired and averaged. In the transmission-based setup, the angular misalignment has been intentionally induced in steps of 0.1 mm vertical displacements, using a precision translational stage, to estimate the correct position of the spectrometer and source (Fig. 1).

In the reflection-based setup with bulk mirror, this obstacle of proper alignment of the source-optical fiber and optical fiber-detector has been removed by connecting the sensor probe with bifurcated fiber bundle (Fig. 2).

In the reflection-based setup with Ag mirror coated SPR probe, the probes have been positioned in vertical

Table 1 The first set of samples list used as sensing layer.

Water–glycerol	Concentrations % V/V	Concentrations wt. % (20°C) ρ glycerol = 12,619 (g/mL)	RI (589 nm, 20°C)
Pure water	—	—	1.333
50–5 mL	9.09%	11.20%	1.346 ($+13 \times 10^{-3}$ RIU)
50–10 mL	16.66%	20.15%	1.357 ($+24 \times 10^{-3}$ RIU)

Table 2 The second set of samples list used as sensing layer.[33]

Sugar concentrations % (W/v)	RI (589 nm, 20°C)
Pure water	1.333
10	1.347
15	1.355
20	1.363
25	1.372

displacement stand and dipped within experimental solution as used in the previous two setups (Fig. 4).

The environmental temperature has been kept constant throughout the experiments.

4 Results and Discussion

4.1 Transmission-Based Setup: Repeatability of Sensor

Figure 5 shows that the resonance wavelength of a particular sample for different experiments is almost the same, which defines significant repeatability of the sensor for the three different solutions. The transmittance spectra obtained for pure water are fitted using a Lorentzian function to get the accurate minimum position of the curve or SPR dip resonance wavelength as shown in Fig. 5 (inset). These analyses represent that there is a redshift of the wavelength with an increasing RI of the sensing layer or analyte.

4.2 Transmission-Based Setup: Long-Term Monitoring of the Sensor

The long-term monitoring of the device has been carried out for a 17 h duration within pure water. By analyzing the SPR dip for each graph collected within 17 h, the variation of the SPR dip wavelength with time is shown in Fig. 6. There is a maximum 1 nm wavelength shift in long-time monitoring, which depicts satisfactory stability of the sensor.

4.3 Transmission-Based Setup: Effect of the Source Misalignment on the Surface Plasmon Resonance Dip
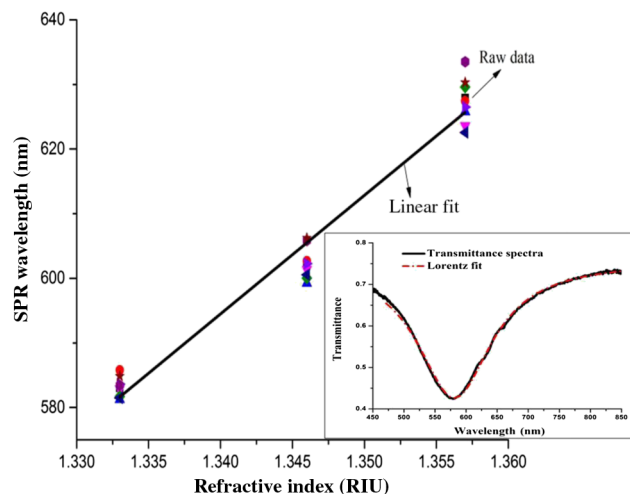
The developed system uses large MMF to provide mechanical rigidity to the probe and to simplify its replacement. A good compromise between sensitivity and connection tolerances is the use of MMFs with a diameter up to few hundred micrometers,[34] but the impact of slight misalignments due to mechanical tolerances has to be evaluated. The misalignment of the setup has been done in our interest with vertical displacement of the LED source to understand if there is any effect of misalignment in SPR curve during real-time monitoring.

Fig. 5 The resonance wavelength variation with RI; inset shows Lorentz fitting of transmittance spectra.

Fig. 6 The SPR wavelength versus time variation for transmittance-based setup.

The outcome of the experiment for pure water is shown in Fig. 7. It shows that there is a decrement in the SNR of the SPR curve and highlights that the SPR dip is clearly visible down to a 0.5 mm misalignment, but with a redshift of ~19 nm, which corresponds to ~10^{-2} RIU, a value unacceptable in most applications. So, it is necessary to change the setup without any alignment procedure.

4.4 Determination of Sensing Parameters

The sensitivities of one particular device for 1.333 RI are 1450, 1380, 1420, 1410, 1290, 1460, and 1430 nm/RIU, the sensitivities for 1.346 RI are 1900, 1890, 1780, 2040, 2210, 1910, and 1730 nm/RIU, and the sensitivities for 1.357 RI are 2340, 2240, 2410, 2680, and 2500 nm/RIU, respectively, at different cycles of experiment. It is clear from the results that the sensitivities of the device are increasing with increase of the external RI. Similarly, the SNR of the device is found to be 4.00357, 4.231157, and 4.28021 for 1.333, 1.346, and 1.357 RI, respectively, from Eq. (3). The
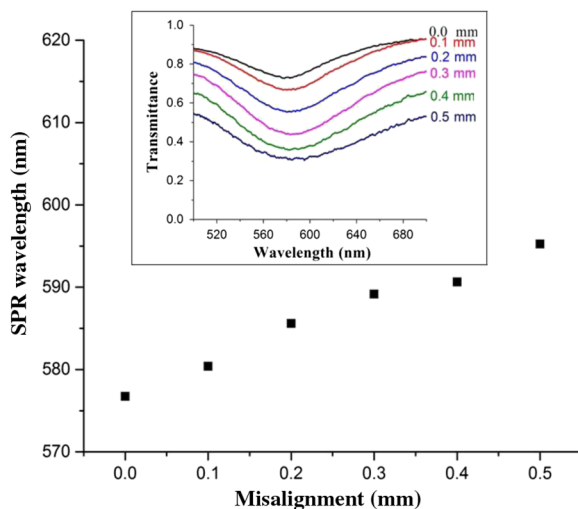
resolutions of the device are 2.166×10^{-4}, 1.580×10^{-4}, and 1.117×10^{-4} for 1.333, 1.346, and 1.357 RI, respectively. The performance parameters for the sensor for external RI of 1.357 and evaluated parameters for whole blood (RI = 1.371) are given in Table 3.
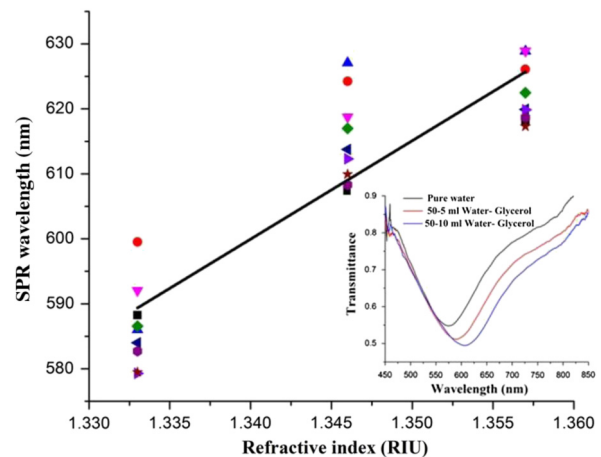
4.5 Reflection-Based Setup with Bulk Mirror: Alignment-Free, Improved Sensitivity

The transmittance curve has been obtained from reflection-based setup through one cycle of experiment with the same sample solution and fiber as used in earlier experiments as shown in the inset of Fig. 8. The SPR wavelength shift versus RI curve is shown in Fig. 8, where a sharp redshift of the wavelength can be noticed. From Eq. (2), the sensitivities of the same gold-coated fiber for transmission- and reflection-based setups are determined and are shown in Fig. 9. It is established that the sensitivities have improved by reflection-based setup.

The reason for the sensitivity improvement can be easily explained. The light wave propagated through the sensing length travels the path of the sensing region two times. Hence, the generated evanescence wave may get a better opportunity to interact with the metal–dielectric (analyte) interface, which is the cause of improved sensitivity of the reflection-based setup. The sensitivities of the gold-coated fiber are 857.17, 1049.39, and 1241.61 nm/RIU for 1.333, 1.346, and 1.357 RI, respectively, for the transmission-based setup, and the improved sensitivities of the same fiber are 1074.34, 1172.03, and 1269.72 nm/RIU, respectively, for the same sample in the case of the reflection-based setup. This shows better performance of the reflection-based setup than the transmission-based one.

Table 3 The variation of sensing parameters with RI.

RI	Resolution (RIU)	Resonance wavelength (nm)	SNR	Sensitivity (nm/RIU)	FWHM (nm)
1.357	1.117×10^{-4}	626.491	4.280	2410	156.827
1.371 (RI of whole blood)	1.051×10^{-4}	651.867	3.828	2850	170.267

Fig. 7 The shifts of the SPR dip as a function of misalignment; inset shows the transmittance spectra.
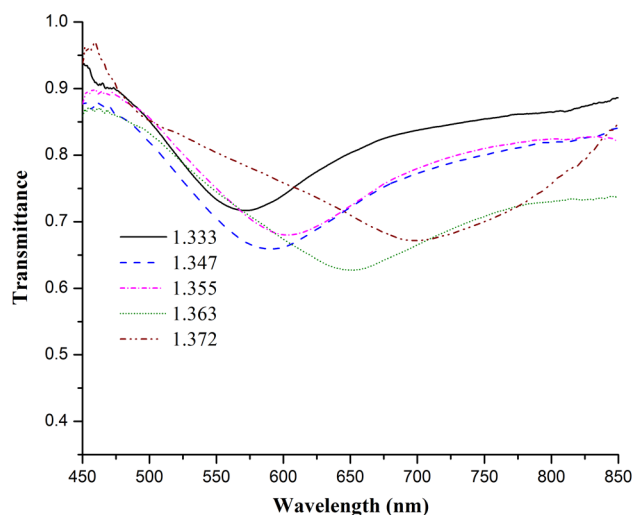

Fig. 8 The SPR wavelength with RI for different cycle of experiment and transmittance spectra (inset), for reflection-based setup.
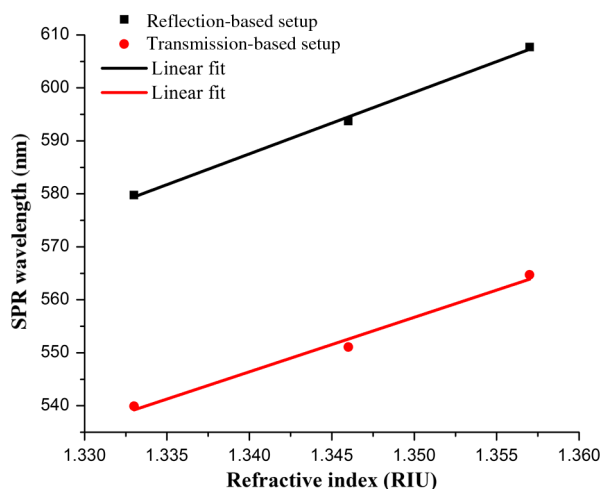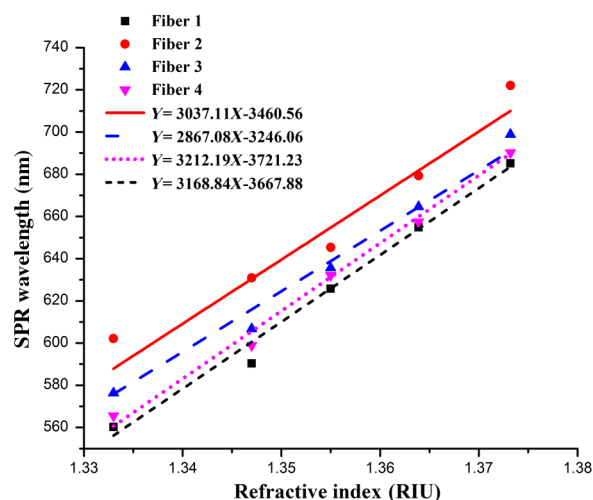
Fig. 9 The SPR wavelength comparison between transmission- and reflection-based setup.

Fig. 11 The SPR wavelength variation with RI for Ag mirror coated SPR probe.

4.6 Reflection-Based Setup with Ag Mirror Coated Probe: Disposable, High Sensitivity

Figure 10 shows the transmittance spectra of one of the Ag mirror coated SPR probe where a sharp redshift is very clear with an increasing RI, which is coupled with the broadening of the SPR spectrum. The SPR wavelength variation with RI is shown in Fig. 11 and the slopes of the fitted lines represent the sensitivity of the SPR probes, which are in the high range as 2867.08, 3037.11, 3168.84, and 3212.19 nm/RIU. High reflectance of the Ag mirror is one of the significant reasons of improved high sensitivity of the gold-coated MMF SPR probe as shown in Fig. 3. Higher reflectance means a satisfactory amount of light can reflect from the mirror and can interact with the surrounding analyte. Lower reflectance should decrease the possibilities of this type of interaction. The bifurcated fiber bundle is a device where launching and receiving light path are different, which introduces less chance of loss of light unlike other optical systems, where a portion of the energy is reflected back into the

source component due to change in the index of refraction. In the visible range of light, the RI of human deoxygenated and oxygenated hemoglobin is in the range of 1.333 to 1.372, which is similar to the detection ability of the proposed Ag mirror coated SPR probe. The values of SNR of particular Ag mirror coated SPR probe for 1.333, 1.347, 1.355, 1.369, and 1.372 RI are 4.649, 4.373, 4.684, 4.429, and 2.001, respectively. The resolutions of the different Ag mirror coated SPR probes are 1.046×10^{-4}, 9.878×10^{-5}, 9.467×10^{-5}, and 9.339×10^{-5}, respectively. By analyzing the SPR dip for each graph collected within 17 h in the reflection-based setup, the variation of the SPR dip wavelength with time is shown in Fig. 12. There is a maximum of 0.5 nm wavelength shift in long-time monitoring, which depicts advanced stability of the sensor than the transmission-based setup. It is very interesting that the sensor is reversely repeatable. In the experiment, the RI has been changed from higher to lower RI and blueshift of the wavelength has been noticed.

Fig. 10 The transmittance spectra of one of Ag mirror coated SPR probe.
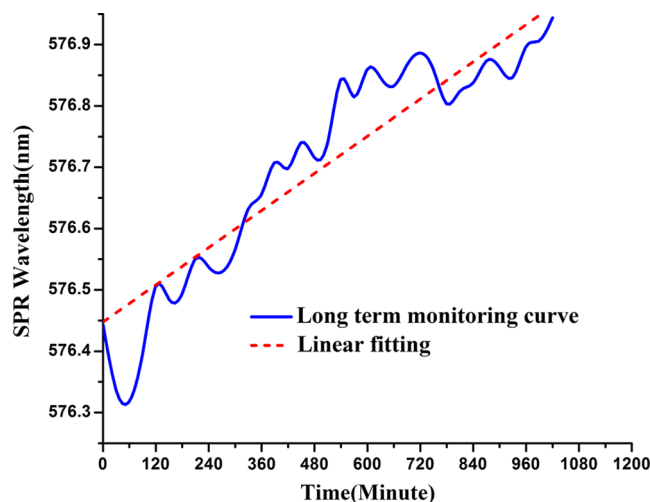
Fig. 12 The SPR wavelength versus time variation for reflectance-based setup.

5 Conclusions

In summary, fabrication and characterization of a sensitive gold-coated optical fiber reflection-based SPR biosensor have been demonstrated as a replacement of transmittance-based sensor with better sensitivity. The sensitivity for whole blood has been predicted as 2850 nm/RIU with RI of 1.371. An effort for the enhancement of the sensor sensitivity in reflection-based setup has also been made by using bifurcated fiber bundle and mirror at distal end of the fiber. The undesired misalignment perturbation has been removed in the reflection-based setup. The sensitivity is improved from 857.17 to 1074.34 nm/RIU by the same fiber for pure water. In the present work, a highly sensitive SPR probe with Ag mirror coated on the fiber tip has been developed with a sensitivity of 3212.19 nm/RIU in the RI range of 1.33 to 1.37. The simplicity and low cost of the technique can be easily employed to fabricate biochemical sensor based on other optically transparent polymer materials. Hence, the proposed SPR probe can bring benefits to the real-time biomedical application.

References

1. A. D. Kersey, "A review of recent developments in fiber optic sensor technology," *Opt. Fiber Technol.* **2**(3), 291–317 (1996).
2. B. H. Lee et al., "Interferometric fiber optic sensors," *Sensors* **12**(3), 2467–2486 (2012).
3. P. Dhara and V. K. Singh, "Effect of MMF stub on the sensitivity of a photonic crystal fiber interferometer sensor at 1550 nm," *Opt. Fiber Technol.* **21**, 154–159 (2015).
4. R. K. Gangwar and V. K. Singh, "Refractive index sensor based on selectively liquid infiltrated dual core photonic crystal fibers," *Photonics Nanostruct. Fundam. Appl.* **15**, 46–52 (2015).
5. R. K. Gangwar, V. Bhardwaj, and V. K. Singh, "Magnetic field sensor based on selectively magnetic fluid infiltrated dual-core photonic crystal fiber," *Opt. Eng.* **55**(2), 026111 (2016).
6. S. Zheng, M. Ghandehari, and J. Ou, "Photonic crystal fiber long-period grating absorption gas sensor based on a tunable erbium-doped fiber ring laser," *Sens. Actuators B* **223**, 324–332 (2016).
7. S. Zheng, Y. Zhu, and S. Krishnaswamy, "Fiber humidity sensors with high sensitivity and selectivity based on interior nanofilm-coated photonic crystal fiber long-period gratings," *Sens. Actuators B* **176**, 264–274 (2013).
8. S. Zheng et al., "Sensitivity characterization of cladding modes in long-period gratings photonic crystal fiber for structural health monitoring," *Measurement* **72**, 43–51 (2015).
9. S. Zheng, "Long-period fiber grating moisture sensor with nano-structured coatings for structural health monitoring," *Struct. Health Monit.* **14**(2), 148–157 (2015).
10. W. Li, N. H. Zhu, and L. X. Wang, "Brillouin-assisted microwave frequency measurement with adjustable measurement range and resolution," *Opt. Lett.* **37**(2), 166–168 (2012).
11. W. Li et al., "True-time delay line with separate carrier tuning using dual-parallel MZM and stimulated Brillouin scattering-induced slow light," *Opt. Express* **19**(13), 12312–12324 (2011).
12. R. C. Jorgenson and S. S. Yee, "A fiber-optic chemical sensor based on surface plasmon resonance," *Sens. Actuators B* **12**(3), 213–220 (1993).
13. Y. Yanase et al., "Surface plasmon resonance for cell-based clinical diagnosis," *Sensors* **14**(3), 4948–4959 (2014).
14. P. Dhara et al., "Design and fabrication of disposable plasmonic fiber probes for biosensing," *Proc. SPIE* **9317**, 93170T (2015).
15. P. Bhatia and B. D. Gupta, "Fabrication and characterization of a surface plasmon resonance based fiber optic urea sensor for biomedical applications," *Sens. Actuators B* **161**(1), 434–438 (2012).
16. K. Takagi and K. Watanabe, "Near infrared characterization of hetero-core optical fiber SPR sensors coated with Ta_2O_5 film and their applications," *Sensors* **12**(2), 2208–2218 (2012).
17. N. Cennamo et al., "Low cost sensors based on SPR in a plastic optical fiber for biosensor implementation," *Sensors* **11**(12), 11752–11760 (2011).
18. C. Fallauto, G. Perrone, and A. Vallan, "Differential surface plasmon resonance sensor for the detection of chemicals and biochemical," *Key Eng. Mater.* **543**, 310–313 (2013).
19. C. Fallauto et al., "A differential optical sensor for long-term monitoring of chemicals," in *Proc. IEEE Int. Instrumentation and Measurement Technology Conf.*, pp. 620–623, Minneapolis, Minnesota (2013).
20. P. Dhara et al., "Transmission and reflection SPR disposable fibre probes for bio-chemical sensing," in *Int. Conf. of Biophotonics*, IEEE, Florence, Italy (2015).
21. H. H. Jeong et al., "Real-time label-free immunoassay of interferon-gamma and prostate-specific antigen using a fiber-optic localized surface plasmon resonance sensor," *Biosens. Bioelectron.* **39**(1), 346–351 (2013).
22. M. H. Tu, T. Sun, and K. T. V. Grattan, "Optimization of gold-nano-particle-based optical fiber surface plasmon resonance (SPR)-based sensors," *Sens. Actuators B* **164**(1), 43–53 (2012).
23. G. Mudhana et al., "Fiber-optic probe based on a bifunctional lensed photonic crystal fiber for refractive index measurements of liquids," *IEEE Sensors J.* **11**(5), 1178–1183 (2011).
24. M. R. Prerana et al., "Design, analysis, and realization of a turbidity sensor based on collection of scattered light by a fiber-optic probe," *IEEE Sens. J.* **12**(1), 44–50 (2012).
25. J. B. Faria, "A theoretical analysis of the bifurcated fiber bundle displacement sensor," *IEEE Trans. Instrum. Meas.* **47**(3), 742–747 (1998).
26. M. C. Moreno-Bondi et al., "Oxygen optrode for use in a fiber-optic glucose biosensor," *Anal. Chem.* **62**(21), 2377–2380 (1990).
27. M. Friebel et al., "Determination of optical properties of human blood in the spectral range 250 to 1100 nm using Monte Carlo simulations with hematocrit-dependent effective scattering phase functions," *J. Biomed. Opt.* **11**(3), 034021 (2006).
28. F. J. Barrera et al., "Optical and spectroscopic properties of human whole blood and plasma with and without Y_2O_3 and $Nd^{3+}:Y_2O_3$ nanoparticles," *Lasers Med. Sci.* **28**(6), 1559–1566 (2013).
29. O. Zhernovaya et al., "The refractive index of human hemoglobin in the visible range," *Phys. Med. Biol.* **56**(13), 4013–4021 (2011).
30. Y. A. Qazwinia et al., "Experimental realization and performance evaluation of refractive index SPR sensor based on unmasked short tapered multimode-fiber operating in aqueous environments," *Sens. Actuators A* **236**, 38–43 (2015).
31. M. Kanso, S. Cuenotand, and G. Louarn, "Sensitivity of optical fiber sensor based on surface plasmon resonance: modeling and experiments," *Plasmonics* **3**(2), 49–57 (2008).
32. J. Cao et al., "Cross-comparison of surface plasmon resonance-based optical fiber sensors with different coating structures," *IEEE Sens. J.* **12**(7), 2355–2361 (2012).
33. R. L. David, *Handbook of Chemistry & Physics*, 64th ed., CRC, Boca Raton, Florida (1984).
34. C. Fallauto, G. Perrone, and A. Vallan, "Impact of optical fiber characteristics in SPR sensors for continuous glucose monitoring," in *Proc. IEEE Int. Symp. on Medical Measurements and Applications* (2014).

Papiya Dhara received her master of science degree in applied physics from the Indian School of Mines, Dhanbad, India, in 2011, where she is currently pursuing her PhD in the same field. She was an Erasmus Mundus Areas+ fellow for one year at Politecnico di Torino, Turin, Italy. Her current research interests include the applications of optical fibers to sensors.

Vinod Kumar Singh received his PhD in applied physics from the Department of Applied Physics, Indian School of Mines, Dhanbad, India. He is currently an associate professor of the Department of Applied Physics, Indian School of Mines, Dhanbad, India. His current research interests include optical fiber sensors and optical fiber lasers, electronics, and photonic crystal fiber. He is a professional life member of the Indian Society for Advancement of Materials and Process Engineering.

Massimo Olivero received his PhD in electronic engineering from the Department of Electronics and Telecommunications, Politecnico di Torino in 2005. He was a visiting scientist in the Technical University of Denmark, Universidade Federal de Pernambuco for several years. His current research interests include optical fiber sensors and optical fiber lasers, femtosecond laser processing, and optical coherence tomography.

Guido Perrone received his PhD in electromagnetic from Politecnico di Torino, Torino, Italy, where he is currently a professor of microwaves and optical fibers and components. His current research interests include fiber optic sensors and high-power fiber lasers. He is a member of IEEE/MTTS, the IEEE/Photonics Society, and the Optical Society of America.